Artificial Intelligence-Enhanced Digital Twin System for a New Generation of Intelligent Battery Management

Fatemeh ShakeriHosseinabad[†,*], Behrouz Far[†,*] , Hamidreza Zareipour[†,*]
[†] Department of Electrical and Software Engineering, University of Calgary, 2500 University Drive NW, Calgary, T2N 1N4, Alberta, Canada

Abstract

Battery management systems are essential to estimate internal battery states and regulate current safely under nonlinear dynamics, noisy sensing, and changing operating regimes. We propose a closed-loop digital-twin–AI framework that integrates (i) a physics-informed neural network (PINN) observer for real-time state estimation, (ii) a high-fidelity single-particle-model digital twin, and (iii) a reinforcement learning (RL) controller that optimizes discharge current under different C-rates. The digital twin provides physically consistent trajectories and synthetic supervision, while the PINN provides a low-latency state of charge (SOC) and state of health (SOH), from noisy measurements, allowing the RL agent to act with realistic partial observability. We evaluated the framework at different C-rates, for both a single cell and a pack of cells. In addition, we include a particle swarm optimization capacity-identification module as an independent SOH benchmark. The results demonstrate stable AI-driven SOC regulation across C-rates and scalable extension from cell-to pack-level monitoring. Furthermore, this approach demonstrates a clear pathway to enhance capacity-based SOH estimation accuracy through richer physics integration and expanded training coverage.

Keywords: Battery Management System, Optimization, Physics Informed Neural Network, Digital Twin, Reinforcement Learning, Artificial Intelligence

1. Introduction

Battery management systems (BMSs) play a key role in ensuring safe, efficient, and long-life operation of battery energy storage systems (BESSs), but face several critical challenges [1, 2]. These challenges are becoming more pronounced as electric vehicles (EVs) and the large-scale integration of solar and wind generation increase the reliance on rechargeable BESSs in both transport [3] and grid applications [4, 5]. In this increasingly demanding context, conventional BMSs often struggle to accurately predict battery behavior under dynamic load profiles [6]. The difficulty is amplified by coupled and nonlinear electrochemical, thermal [7], and mechanical processes that can trigger safety-critical failure mechanisms [8, 9]. These limitations motivate AI-enabled predictive BMS frameworks that can handle complex dynamics and safety-critical scenarios [10, 11]. Consequently, a new generation of machine-learning-based BMSs has emerged [12, 13], with the aim of improving the real-time estimation of key states such as SOC and SOH, and to allow more effective charge–discharge control for degradation and safety mitigation [14, 15].

Early ML-based BMSs relied on classical models such as k-nearest neighbors (KNN) [16] and support vector machines (SVMs) [17]. Although promising, these methods face limitations under high-dimensional sensing, stringent real-time constraints, and the need for extensive feature engineering [18]. This has accelerated a shift to deep learning (DL), which can learn nonlinear mappings and automate feature extraction, thus supporting more accurate and adaptive BMS functionality [19, 20]. In this paper, we emphasize that AI is not an add-on to classical estimation; rather, it provides a scalable mechanism to fuse

[*]Fatemeh.Shakerihosse@ucalgary.ca
[*]far@ucalgary.ca
[*]hzareipo@ucalgary.ca

heterogeneous measurements and operational context into actionable state estimates that can improve monitoring and control in real-world BESS deployments [21, 22].

In parallel, digital twin (DT) technology has emerged as a powerful paradigm for battery management [23, 24]. A battery DT combines high-fidelity models with real-time sensor data, usage history, and environmental information to mirror the performance and aging trajectory of its physical counterpart [25, 26]. DTs have been used for the estimation of SOC and SOH and the prediction of battery performance [26–29], including cloud-based implementations [30] and the prediction of EV energy/range [28, 31].

Existing DT modeling approaches are commonly categorized as physics-based or data-driven [26, 29]. Physics-based electrochemical models (e.g., single particle type models) capture internal states and fundamental processes [32], but can be computationally intensive for real-time use [33, 34]. Data-driven models such as neural networks [35–37], and statistical approaches are efficient and scalable [38–40], but may require large datasets, can fail outside the training envelope, and often lack physical consistency [36, 41–43]. These trade-offs motivate hybrid approaches that explicitly integrate AI with physics [44, 45], including PINNs [46] that embed governing equations as soft constraints [47–49].

Integrating PINN and Digital Twins with RL offers a high-fidelity, physics-consistent framework for advanced secondary battery management. PINNs-based techniques have demonstrated strong performance in the estimation of SOC and SOH and the extrapolation of degradation under realistic operating conditions [50–52]. The embedding of PINNs in DTs enables physics-consistent virtual batteries that can operate in real time [53, 54], despite ongoing computational challenges [55, 56]. Moreover, optimal operation requires adaptive decision-making; RL has gained traction for sequential battery control in EV and grid-scale settings [57, 58]. However, training RL directly on real batteries is infeasible and low-fidelity environments can produce unsafe policies [59, 60], motivating DTs as high-fidelity training environments [26, 27, 29, 54]. Recent work highlights the synergy between PINN-enhanced models and RL [61–64]. In this study we propose a unified framework that systematically integrates Digital Twins, PINNs, and RL; however, such fully integrated PINN–DT–RL architectures for secondary battery systems remain largely unexplored [65].

2. Methodology and Platforms

Figure 1 illustrates the proposed closed-loop, next-generation BMS framework for advanced battery management. The system's operation is initiated by the physical battery and sensors, which continuously acquire real-time data, including voltage (V), current (I), and temperature (T). This real-time data is transmitted to the BMS Controller / Actuators.

From the controller, measurements and commands are forwarded to the Digital Twin, which integrates a physics-based single particle model (SPM) to generate simulation states and physics-consistent constraints. These DT outputs are provided to the PINN, which processes the constrained simulations to estimate the SOC and SOH. The resulting estimates are then passed to the Soft Actor-Critic (SAC)-RL module, which learns optimal control actions (e.g., dynamic current limits) that are sent back to the BMS controller/actuators to regulate battery operation. In parallel, the SAC agent provides optimization parameters to refine DT, creating a feedback loop that adapts to the evolving condition of the battery and supports safe and efficient performance.

This work proposes a hybrid closed-loop framework that combines: (i) a PINN for SOC and SOH estimation, (ii) a high-fidelity SPM digital twin implemented in PyBaMM, and (iii) a SAC agent that optimizes current profiles across different C-rates. In addition, a particle swarm optimization (PSO) [30] module estimates capacity fade from current and SOC trajectories to provide an independent SOH benchmark. All components are implemented in Python using PyTorch (for the PINN) , PyBaMM (SPM twin), Gymnasium (environments), and Stable-Baselines3 (SAC) and are integrated into a unified simulation pipeline.

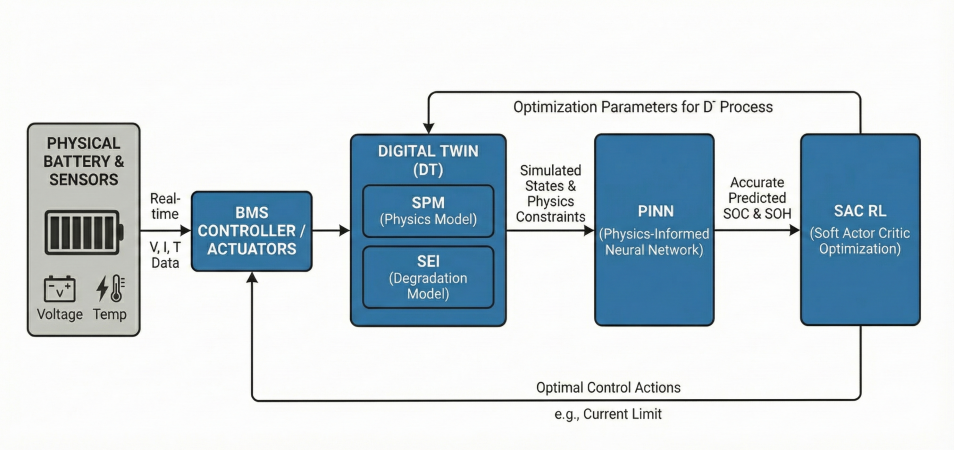

Figure 1. Proposed Closed-Loop Architecture for Advanced Battery Management System leveraging Digital Twin, PINN, and SAC RL.

2.1. **Physics-informed neural network for SOC–SOH prediction**

The PINN is designed as a compact feed-forward network that takes as input the estimated SOC, current, and terminal voltage at time k, and outputs the predicted SOC and SOH at time $k+1$, as defined in Equation (2.1). The architecture consists of two hidden layers with tanh activations and an output layer with bounded nonlinearities to enforce physically meaningful ranges:

$$\hat{SOC}_{k+1} = \sigma(\cdot) \in [0,1], \qquad \widehat{SOH}_{Q,k+1} = 1.1\,\sigma(\cdot) \tag{2.1}$$

where $\sigma(\cdot)$ denotes the logistic sigmoid function.

Training is based on a physics-informed loss that combines data fidelity with Coulomb-counting consistency. For each supervised batch (x_k, y_{k+1}), the loss is given by Equation (2.2):

$$\mathcal{L} = \underbrace{\left\|\hat{\mathrm{SOC}}_{k+1} - \mathrm{SOC}_{k+1}\right\|_2^2 + \left\|\widehat{\mathrm{SOH}}_{Q,k+1} - \mathrm{SOH}_{Q,k+1}\right\|_2^2}_{\text{data loss}} + \lambda_{\text{phys}} \underbrace{\left\|\hat{\mathrm{SOC}}_{k+1} - \tilde{\mathrm{SOC}}_{k+1}^{\mathrm{CC}}\right\|_2^2}_{\text{physics loss}} \tag{2.2}$$

where $\tilde{\mathrm{SOC}}_{k+1}^{\mathrm{CC}}$ is the SOC predicted by discrete Coulomb counting using the predicted capacity as defined in Equation (2.3)

$$Q_{\text{hat}} = Q_{\text{nom}} \cdot \widehat{\mathrm{SOH}}_{Q,k+1}, \qquad \tilde{\mathrm{SOC}}_{k+1}^{\mathrm{CC}} = \mathrm{SOC}_k - \frac{I_k\,dt}{3600\,Q_{\text{hat}}} \tag{2.3}$$

The weighting parameter λ_{phys} balances the data fitting against the adherence to the physical conservation law. Optimization is carried out using the Adam optimizer over multiple epochs in the training dataset.

2.2. **SPM digital twin and PINN-based online estimator**

The SPM is configured with default parameter values and is solved with PyBaMM's time-stepping solver. A pre-discharge step at a fixed C-rate is used to initialize the cell near a target SOC (e.g. 0.9).

In closed-loop environments, the SPM is treated as the ground-truth digital twin. At each time step, the following operations are performed;

(1) Applies a discharge current I_k and advances the SPM by dt,

(2) Extracts the true SOC from the SPM solution (using capacity-based or concentration-based definitions) and the terminal voltage V_k,
(3) Corrupts V_k with Gaussian noise to obtain a pseudo-measurement V_k^{meas},
(4) Passes $(\hat{\text{SOC}}_k, I_k, V_k^{\text{meas}})$ through the trained PINN estimator to obtain $(\hat{\text{SOC}}_{k+1}, \widehat{\text{SOH}}_{Q,k+1})$.

The PINN is wrapped as an online estimator whose internal state $(\hat{\text{SOC}}, \widehat{\text{SOH}}_Q)$ is updated at each step. Thus, the SAC agent observes an estimated internal state derived from AI, rather than the exact SPM state, mimicking the partial observability of a real BMS.

2.3. **Reinforcement learning environment and SAC control**

To design control policies, we formulate a Gymnasium-compatible environment in which the agent interacts with the SPM+PINN loop. In the training environment (fresh cell), the observation at time k is stated in equation 2.4.

$$\mathbf{o}_k = \left[\hat{\text{SOC}}_k,\ \widehat{\text{SOH}}_{Q,k},\ V_k^{\text{meas}},\ I_{k-1}\right] \tag{2.4}$$

and the action is a continuous discharge current $a_k = I_k \in [0, I_{\max}]$. The reward function penalizes SOC deviation from a target value and excessively large currents, with additional negative reward and termination when voltage or SOC leave safe operating bounds. The duration of the episode is limited (e.g. 600 s), emulating finite driving or dispatch intervals.

For each target C-rate $C \in \{0.5, 1.0, 2.0\}$, we set $I_{\max} = C \cdot Q_{\text{SPM}}$ (where Q_{SPM} is the SPM nominal capacity) and train a separate SAC policy. This yields policies adapted to different power levels while consistently using PINN-based estimates as input.

2.4. **Aging environment and PSO-based capacity SOH estimation**

To study SOH tracking under degradation, we construct a second SPM environment that includes an explicit capacity-fade model. In this *aging* environment, the true capacity $Q_{\text{true}}(t)$ decays over time. The SPM SOC computation uses $Q_{\text{true}}(t)$, producing a ground-truth SOH trajectory stated with equation 2.5.

$$\text{SOH}_{Q,\text{true}}(t) = Q_{\text{true}}(t)/Q_{\text{nom}}. \tag{2.5}$$

The PINN estimator is left unchanged, so any mismatch between its internal SOH representation and the true SOH reflects both modeling and estimation limitations. In parallel, we implement a PSO-based capacity identification scheme to provide an additional SOH estimate directly from SPM output.

2.5. **Multi-C-rate closed-loop experiments**

For each C-rate $C \in \{0.5, 1.0, 2.0\}$, the resulting trajectories allow us to compare: (i) the SAC-controlled SOC tracking across C-rates, (ii) the PINN-based SOH estimates against the ground-truth SOH and the PSO-based capacity SOH, and (iii) the impact of C-rate on degradation and control effort. SOC and SOH time series, together with current profiles, are plotted for qualitative analysis.

3. **Results**

This section analyzes the closed-loop behaviour of the proposed PINN–DT–SAC BMS framework over a 600 s discharge horizon at three rates, 0.5C, 1C, and 2C. Results are presented for both a single battery cell and a multi-cell battery pack.

3.1. **Closed-loop SOC regulation**

Fig. 2 shows the SOC trajectories for the three C-rates. In each case, the true SOC obtained from the SPM decreases approximately linearly from an initial value close to 0.9 as the cell is discharged. The slope becomes steeper with increasing C-rate, as expected: at 0.5C the true SOC only drops a few percent over 600 s, whereas at 2C it approaches the lower bound of the operating window.

The PINN-based estimate exhibits a fast transient during the first tens of seconds, followed by a quasi-steady regime in which the estimated SOC remains close to a narrow band slightly above the target SOC of 0.8 (dotted line). For all three C-rates, the agent, which observes only the estimated SOC and SOH, learns to initially apply a relatively high current and then regulate the current so that $\hat{\text{SOC}}$ stays within ≈ 0.82–0.84. This behavior is consistent in 0.5C, 1C, and 2C, indicating that the SAC policy is generalized across different power levels.

However, the gap between SOC_{true} and SOC_{hat} increases with the C-rate. At 0.5C, the estimated SOC slightly overestimates the true SOC, but the offset remains modest. At 2C, the true SOC drifts further away from the target line, while the estimator maintains a nearly constant value. This is a direct consequence of the fact that the agent acts in the estimated state; as long as $\hat{\text{SOC}}$ is kept near the target, the controller is unaware of the additional depletion visible only in the SPM state. These results show that the AI-based controller is capable of stabilizing the estimated SOC around the target band across multiple C-rates.

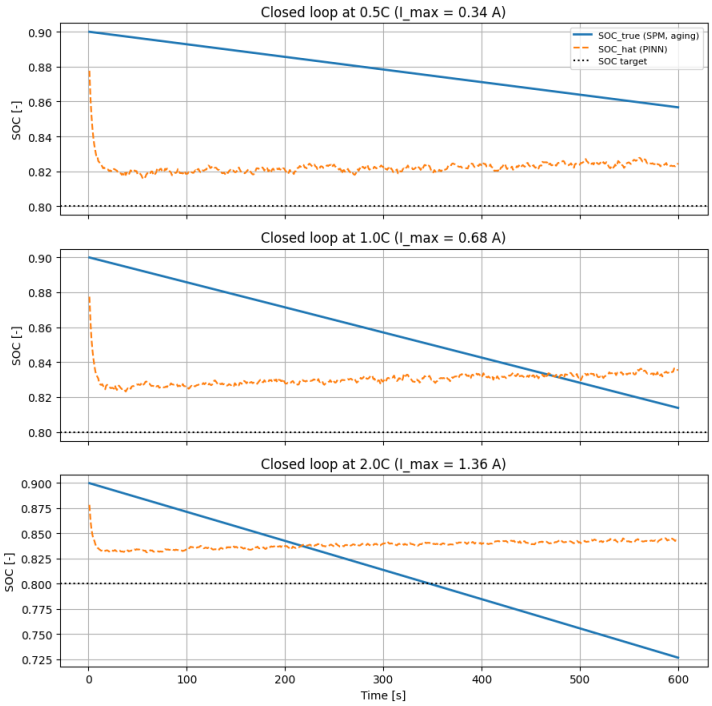

Figure 2. Single-cell closed-loop SOC trajectories under three discharge rates (0.5C, 1C, and 2C) over a 600 s horizon. The solid line shows the digital-twin ground truth SOC_{true} (SPM with aging), the dashed line shows the PINN estimate $\widehat{\text{SOC}}$, and the dotted line indicates the SOC target. The corresponding current limits are $I_{\max} = 0.34$ A (0.5C), 0.68 A (1C), and 1.36 A (2C).

3.2. **SOH trajectories and estimator comparison**

Figure 3 presents the corresponding SOH trajectories for the same three C-rates. The solid blue curve represents the ground-truth capacity-based SOH injected into the SPM environment through the prescribed aging law. Over the 600 s window, the true SOH remains close to unity at 0.5C and 1C, with only a very mild decline. At 2C, the decay is more pronounced, with visible steps as the discrete-time aging model reduces the effective capacity.

The green dotted curve shows the SOH estimated by the PSO-based capacity identification method. Across all C-rates, the PSO estimate tracks the true SOH trajectory very closely; the two curves are nearly indistinguishable at 0.5C and 1C and only show a small lag or smoothing at 2C due to the finite window length used in optimization. This behavior confirms that, given a sufficiently informative current and SOC trajectory, the PSO scheme can recover the effective capacity with high accuracy.

In contrast, the orange dashed curve, SOH obtained from PINN remains almost constant around ≈ 0.93 for all three C-rates and exhibits only small fluctuations around this value. The proposed PINN demonstrates stability in the estimation of SOH, maintaining a consistent trajectory throughout the episode. The observed deviation from the true SOH at 2C highlights the sensitivity of the model to the training data distribution. This indicates a promising avenue for enhancing the model's predictive capability by incorporating more diverse aging scenarios into the training phase.

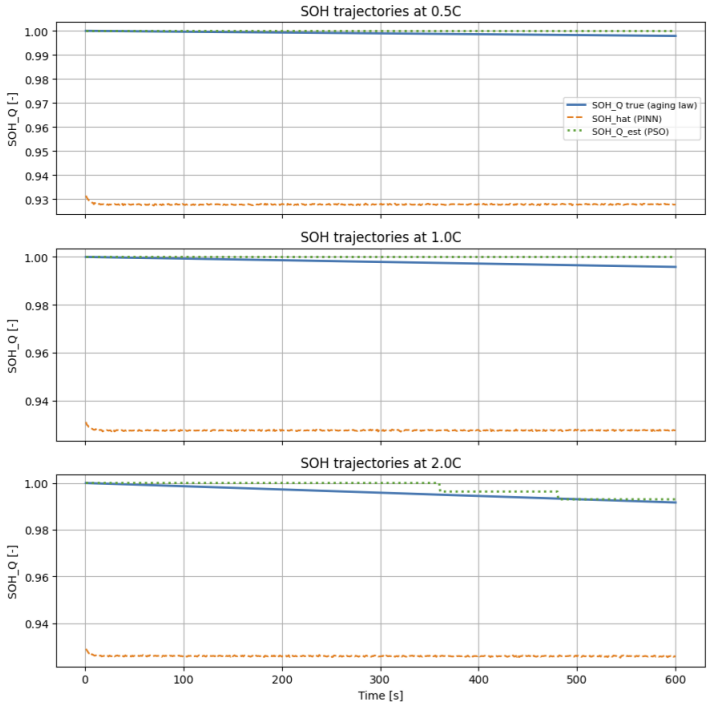

Figure 3. Single-cell SOH trajectories under three discharge rates (0.5C, 1C, and 2C) over a 600 s horizon. The solid curve shows the ground-truth health $\mathrm{SOH}_{Q,\mathrm{true}}$ from the aging law, the dashed curve shows the PINN estimate $\widehat{\mathrm{SOH}}$, and the dotted curve shows the independent capacity-fade estimate $\mathrm{SOH}_{Q,\mathrm{est}}$ obtained with PSO.

Figures 4 and 5 report pack-mean SOC and SOH trajectories over a 600 s discharge at 0.5C, 1C, and 2C using an SPM-based digital twin for each cell. The digital twin produces physically consistent behavior, with the SOC decreasing monotonically and exhibiting the

expected dependence on the C-rate (faster depletion at a higher C-rate). Over this short horizon, the true SOH remains close to unity, which is consistent with the slow time scale of capacity-fade mechanisms relative to a 10-minute experiment. These trends provide a reliable physics-grounded reference for validating estimation performance and for building pack-level metrics (mean/min, imbalance) required by BMSs.

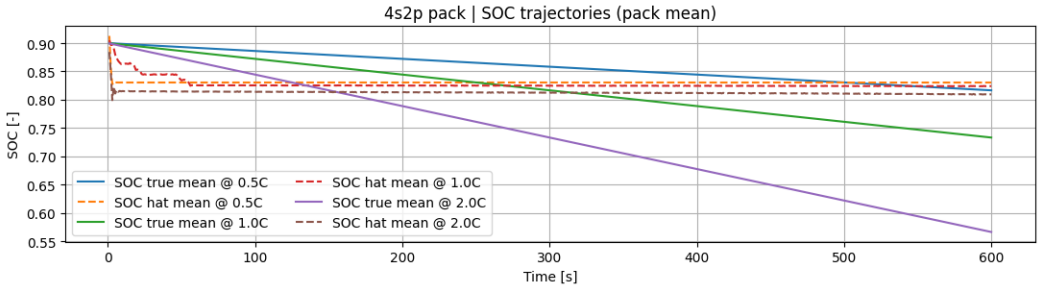

Figure 4. Pack-mean SOC trajectories for a 4s2p battery pack over a 600 s discharge at three rates (0.5C, 1C, and 2C). Solid curves show the digital-twin ground truth $\mathrm{SOC}_{\mathrm{true,mean}}$, while dashed curves show the PINN-based estimates $\widehat{\mathrm{SOC}}_{\mathrm{mean}}$, both averaged across all cells in the pack.

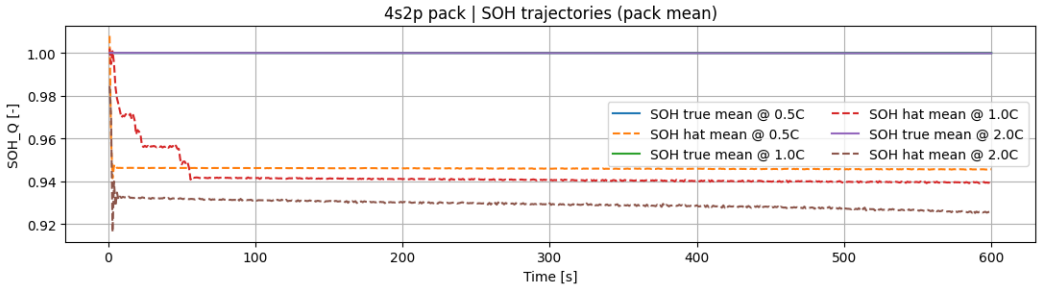

Figure 5. Pack-mean SOH trajectories for a 4s2p battery pack over a 600 s discharge at three rates (0.5C, 1C, and 2C). Solid curves show the digital-twin ground truth $\mathrm{SOH}_{Q,\mathrm{true,mean}}$ from the aging law, while dashed curves show the PINN-based estimates $\widehat{\mathrm{SOH}}_{\mathrm{mean}}$, both averaged across all cells in the pack.

4. **Discussion**

The closed-loop experiments highlight both the potential and the limitations of the proposed AI-driven framework. From a control perspective, the SAC agent, which operates purely on PINN-based estimates and noisy voltage measurements, successfully learns a policy that maintains the estimated SOC close to a desired setpoint across different C-rates. This demonstrates the feasibility of using deep RL to plan current trajectories under partial observability, and shows that a single architecture can generalize across operating regimes when appropriately trained. From an estimation perspective, the results are more nuanced. The PINN achieves stable, low-variance SOC estimates that are well aligned with the control objective and remain within physically admissible bounds.

The PSO-based SOH estimator provides a useful counterpoint. It requires a sliding window of data and is computationally heavier, but it can accurately recover the effective capacity trajectory in the SPM aging environment. In the present framework, the PSO method serves as an *external benchmark* for evaluating learned SOH estimates: the agreement between $\mathrm{SOH}_{Q,\mathrm{True}}$ and $\mathrm{SOH}_{Q,\mathrm{est}}$ (PSO) confirms that the aging law and the implementation

of the SPM are consistent, the discrepancy with $\widehat{\mathrm{SOH}}$ (PINN) serves as a useful diagnostic signal, guiding targeted improvements to align the AI estimator with a physically calibrated health model. These findings have several important implications as follows:

(1) The combination of PINN-based SOC estimation and RL control is promising for real-time BMS applications because it provides fast, differentiable, and noise-robust estimates that can be tightly integrated into AI planning algorithms.
(2) For capacity-based SOH, additional physics (e.g. SEI growth models in PyBaMM), richer training data including long-term cycling and temperature variation, or multi-task architectures may be required.
(3) Hybrid strategies, in which a fast learned estimator (PINN) is periodically corrected by a slower but more accurate optimizer (PSO or Bayesian filters), appear particularly attractive. The present results show that PSO can track true SOH closely, suggesting that a practical system could use PSO-style identification at coarser intervals to recalibrate the PINN or to adapt its SOH output.
(4) From an AI-systems perspective, the behaviour observed at different C-rates underscores the importance of training data coverage and domain adaptation when deploying deep models in cyber-physical settings. The controller performs well as long as the estimator bias is moderate; when estimator bias grows at high C-rate, the closed-loop behavior can deviate from the desired physical trajectory even though the agent believes it is on target.

The key contribution of the AI component is that the PINN observer delivers a low-latency belief state $(\widehat{\mathrm{SOC}}, \widehat{\mathrm{SOH}})$ directly from noisy measurements, enabling digital-twin-informed monitoring and control without repeatedly solving the full electrochemical model online.

Even when estimation gaps appear, the AI–twin coupling remains valuable because it provides immediate, quantitative diagnostics of where the learned observer must be strengthened. For SOC, this points to the need for improved temporal consistency in observer estimates. For SOH, it highlights the importance of better identifiability and stronger regularization, which together accelerate iteration toward a robust closed-loop BMS.

In this sense, the framework demonstrates a practical pathway in which *AI augments physics*; the digital twin supplies trustworthy dynamics and synthetic supervision, while the PINN supplies fast state inference and a scalable interface for pack-level decision-making across operating conditions.

4.1. **Limitations and future work**

The current implementation has several limitations that should be acknowledged. First, real degradation mechanisms are more complex, involving path-dependent side-reactions, temperature effects, and calendar aging. Incorporating physics-based degradation models in PyBaMM and training on data generated from such models, or from experimental cycling campaigns, would provide a more faithful test of SOH tracking capabilities.

Moreover, the RL controller is trained a fixed SOC target. In practice, operators typically seek to optimize multi-objective criteria such as round-trip efficiency, cycle life, power availability, and safety margins, possibly subject to time-varying electricity prices or grid constraints. Multi-objective RL formulations and constrained RL methods could provide policies that better reflect real-world decision trade-offs and improve interpretability, particularly when coupled with physics-consistent and explainable PINN-based SOC/SOH estimators. The present work does not include an explicit comparison with alternative SOH estimation techniques such as Kalman-filter-based observers. Such baselines would provide quantitative evidence of the benefits of the proposed PINN-based estimator. These directions are left for future research and will be essential for positioning the proposed integrated PINN–DT–RL framework within the broader battery management literature.

5. Conclusion

This work demonstrates an integrated digital-twin–AI pathway toward next-generation battery management by combining a high-fidelity SPM digital twin, a PINN observer, and an SAC control policy in a unified closed-loop pipeline. Across multi-rate discharge experiments and for both single-cell and 4s2p package settings, the proposed integrated architecture achieves stable, health-aware SOC regulation using AI-based state estimates. The central impact of AI in this study is to enable fast, scalable inference of latent states $(\widehat{\mathrm{SOC}}, \widehat{\mathrm{SOH}})$ from noisy measurements. It also establishes a practical interface for adaptive decision-making without repeatedly solving the entire electrochemical model online, thus supporting real-time BMS operation and extension from cell to pack.

Beyond demonstrating end-to-end feasibility, the results establish a clear and constructive roadmap for strengthening long-horizon health monitoring within the same AI–physics architecture. Future work will enhance the digital twin by incorporating richer degradation physics and broadening its training data to encompass extended cycling horizons and temperature variability. Furthermore, we will integrate hybrid strategies that combine fast-learning estimation with periodic optimization-based recalibration.

These directions will further improve capacity-based SOH identifiability and improve domain robustness while preserving the key advantage of low-latency state estimation enabled by AI. The proposed framework offers a practical foundation for robust, adaptive and AI-enhanced battery management from cell to pack.

Acknowledgements

The authors gratefully acknowledge the funding support provided by the National Research Council of Canada.

References

[1] E. Fan, L. Li, Z. Wang, J. Lin, Y. Huang, Y. Yao, R. Chen, and F. Wu. "Sustainable recycling technology for Li-ion batteries and beyond: challenges and future prospects". In: *Chemical reviews* 120.14 (2020), pp. 7020–7063.

[2] J.-M. Tarascon and M. Armand. "Issues and challenges facing rechargeable lithium batteries". In: *nature* 414.6861 (2001), pp. 359–367.

[3] M. Beaudin, H. Zareipour, A. Schellenberglabe, and W. Rosehart. "Energy storage for mitigating the variability of renewable electricity sources: An updated review". In: *Energy for sustainable development* 14.4 (2010), pp. 302–314.

[4] B. Dunn, H. Kamath, and J.-M. Tarascon. "Electrical energy storage for the grid: a battery of choices". In: *Science* 334.6058 (2011), pp. 928–935.

[5] M. Farrokhabadi, S. König, C. A. Cañizares, K. Bhattacharya, and T. Leibfried. "Battery energy storage system models for microgrid stability analysis and dynamic simulation". In: *IEEE Transactions on Power Systems* 33.2 (2017), pp. 2301–2312.

[6] K. See, G. Wang, Y. Zhang, Y. Wang, L. Meng, X. Gu, N. Zhang, K. Lim, L Zhao, and B. Xie. "Critical review and functional safety of a battery management system for large-scale lithium-ion battery pack technologies". In: *International Journal of Coal Science & Technology* 9.1 (2022), p. 36.

[7] Y. Dai and A. Panahi. "Thermal runaway process in lithium-ion batteries: A review". In: *Next Energy* 6 (2025), p. 100186.

[8] D. P. Finegan, J. Zhu, X. Feng, M. Keyser, M. Ulmefors, W. Li, M. Z. Bazant, and S. J. Cooper. "The application of data-driven methods and physics-based learning for improving battery safety". In: *Joule* 5.2 (2021), pp. 316–329.

[9] C. R. Birkl, M. R. Roberts, E. McTurk, P. G. Bruce, and D. A. Howey. "Degradation diagnostics for lithium ion cells". In: *Journal of Power Sources* 341 (2017), pp. 373–386.

[10] J. M. Reniers, G. Mulder, S. Ober-Blöbaum, and D. A. Howey. "Improving optimal control of grid-connected lithium-ion batteries through more accurate battery and degradation modelling". In: *Journal of Power Sources* 379 (2018), pp. 91–102.

[11] M.-K. Tran, S. Panchal, T. D. Khang, K. Panchal, R. Fraser, and M. Fowler. "Concept review of a cloud-based smart battery management system for lithium-ion batteries: Feasibility, logistics, and functionality". In: *Batteries* 8.2 (2022), p. 19.

[12] M.-K. Tran, S. Panchal, V. Chauhan, N. Brahmbhatt, A. Mevawalla, R. Fraser, and M. Fowler. "Python-based scikit-learn machine learning models for thermal and electrical performance prediction of high-capacity lithium-ion battery". In: *International Journal of Energy Research* 46.2 (2022), pp. 786–794.

[13] V. Klass, M. Behm, and G. Lindbergh. "A support vector machine-based state-of-health estimation method for lithium-ion batteries under electric vehicle operation". In: *Journal of Power Sources* 270 (2014), pp. 262–272.

[14] S. Yang, X. Liu, L. Shen, and C. Zhang. *Advanced battery management system for electric vehicles*. Vol. 1. Springer, 2023.

[15] Y. Wei, M. Wang, M. Zhang, T. Cai, Y. Huang, and M. Xu. "Advancements, Challenges, and Future Trajectories in Advanced Battery Safety Detection". In: *Electrochemical Energy Reviews* 8.1 (2025), p. 10.

[16] C. Hu, G. Jain, P. Zhang, C. Schmidt, P. Gomadam, and T. Gorka. "Data-driven method based on particle swarm optimization and k-nearest neighbor regression for estimating capacity of lithium-ion battery". In: *Applied Energy* 129 (2014), pp. 49–55.

[17] V. Vapnik. "The support vector method of function estimation". In: *Nonlinear modeling: Advanced black-box techniques*. Springer, 1998, pp. 55–85.

[18] Y. Wu, D. Bai, K. Zhang, Y. Li, and F. Yang. "Advancements in the estimation of the state of charge of lithium-ion battery: A comprehensive review of traditional and deep learning approaches". In: *Journal of Materials Informatics* 5.2 (2025), N–A.

[19] D. E. Rumelhart, G. E. Hinton, and R. J. Williams. "Learning representations by back-propagating errors". In: *nature* 323.6088 (1986), pp. 533–536.

[20] J. J. Hopfield. "Neural networks and physical systems with emergent collective computational abilities." In: *Proceedings of the national academy of sciences* 79.8 (1982), pp. 2554–2558.

[21] X. Sui, S. He, S. B. Vilsen, J. Meng, R. Teodorescu, and D.-I. Stroe. "A review of non-probabilistic machine learning-based state of health estimation techniques for Lithium-ion battery". In: *Applied Energy* 300 (2021), p. 117346.

[22] H. A. Gabbar, A. M. Othman, and M. R. Abdussami. "Review of battery management systems (BMS) development and industrial standards". In: *Technologies* 9.2 (2021), p. 28.

[23] Y. Lu, C. Liu, I Kevin, K. Wang, H. Huang, and X. Xu. "Digital Twin-driven smart manufacturing: Connotation, reference model, applications and research issues". In: *Robotics and computer-integrated manufacturing* 61 (2020), p. 101837.

[24] A. Thelen, X. Zhang, O. Fink, Y. Lu, S. Ghosh, B. D. Youn, M. D. Todd, S. Mahadevan, C. Hu, and Z. Hu. "A comprehensive review of digital twin—part 2: roles of uncertainty quantification and optimization, a battery digital twin, and perspectives". In: *Structural and multidisciplinary optimization* 66.1 (2023), p. 1.

[25] E. Glaessgen and D. Stargel. "The digital twin paradigm for future NASA and US Air Force vehicles". In: *53rd AIAA/ASME/ASCE/AHS/ASC Structures, Structural Dynamics and Materials Conference* (2012).

[26] B. Wu, W. D. Widanage, S. Yang, and X. Liu. "Battery digital twins: Perspectives on the fusion of models, data and artificial intelligence for smart battery management systems". In: *Energy and AI* 1 (2020), p. 100016.

[27] A. Thelen, X. Zhang, O. Fink, Y. Lu, S. Ghosh, B. D. Youn, M. D. Todd, S. Mahadevan, C. Hu, and Z. Hu. "A comprehensive review of digital twin—part 1: modeling and twinning enabling technologies". In: *Structural and Multidisciplinary Optimization* 65.12 (2022), p. 354.

[28] F. Tao, M. Zhang, Y. Liu, and A. Y. Nee. "Digital twin in industry: State-of-the-art". In: *IEEE Transactions on Industrial Informatics* 15.4 (2019), pp. 2405–2415.

[29] M. Dubarry, D. Howey, and B. Wu. "Enabling battery digital twins at the industrial scale". In: *Joule* 7.6 (2023), pp. 1134–1144.

[30] W. Li, M. Rentemeister, J. Badeda, D. Jöst, D. Schulte, and D. U. Sauer. "Digital twin for battery systems: Cloud battery management system with online state-of-charge and state-of-health estimation". In: *Journal of energy storage* 30 (2020), p. 101557.

[31] F. Tao, Q. Qi, A. Liu, and A. Kusiak. "Data-driven smart manufacturing". In: *Journal of manufacturing systems* 48 (2018), pp. 157–169.

[32] M. Doyle, T. F. Fuller, and J. Newman. "Modeling of galvanostatic charge and discharge of the lithium/polymer/insertion cell". In: *Journal of the Electrochemical society* 140.6 (1993), p. 1526.

[33] F. Saidani, F. X. Hutter, R.-G. Scurtu, W. Braunwarth, and J. N. Burghartz. "Lithium-ion battery models: a comparative study and a model-based powerline communication". In: *Advances in Radio Science* 15 (2017), pp. 83–91.

[34] A. M. Bizeray, S. Zhao, S. R. Duncan, and D. A. Howey. "Lithium-ion battery thermal-electrochemical model-based state estimation using orthogonal collocation and a modified extended Kalman filter". In: *Journal of Power Sources* 296 (2015), pp. 400–412.

[35] E. Chemali, P. J. Kollmeyer, M. Preindl, and A. Emadi. "State-of-charge estimation of Li-ion batteries using deep neural networks: A machine learning approach". In: *Journal of Power Sources* 400 (2018), pp. 242–255.

[36] K. A. Severson, P. M. Attia, N. Jin, N. Perkins, B. Jiang, Z. Yang, M. H. Chen, M. Aykol, P. K. Herring, D. Fraggedakis, et al. "Data-driven prediction of battery cycle life before capacity degradation". In: *Nature Energy* 4.5 (2019), pp. 383–391.

[37] P. M. Attia, A. Grover, N. Jin, K. A. Severson, T. M. Markov, Y.-H. Liao, M. H. Chen, B. Cheong, N. Perkins, Z. Yang, et al. "Closed-loop optimization of fast-charging protocols for batteries with machine learning". In: *Nature* 578.7795 (2020), pp. 397–402.

[38] W. Choi, H.-C. Shin, J. M. Kim, J.-Y. Choi, and W.-S. Yoon. "Modeling and applications of electrochemical impedance spectroscopy (EIS) for lithium-ion batteries". In: *Journal of Electrochemical Science and Technology* 11.1 (2020), pp. 1–13.

[39] A. Hentunen, T. Lehmuspelto, and J. Suomela. "Time-domain parameter extraction method for thévenin-equivalent circuit battery models". In: *ieee transactions on energy conversion* 29.3 (2014), pp. 558–566.

[40] H Ij. "Statistics versus machine learning". In: *Nat Methods* 15.4 (2018), p. 233.

[41] S. Greenbank and D. Howey. "Automated feature extraction and selection for data-driven models of rapid battery capacity fade and end of life". In: *IEEE Transactions on Industrial Informatics* 18.5 (2021), pp. 2965–2973.

[42] Z. Yun and W. Qin. "Remaining useful life estimation of lithium-ion batteries based on optimal time series health indicator". In: *Ieee Access* 8 (2020), pp. 55447–55461.

[43] M. Raissi, P. Perdikaris, and G. E. Karniadakis. "Physics-informed neural networks: A deep learning framework for solving forward and inverse problems involving nonlinear partial differential equations". In: *Journal of Computational Physics* 378 (2019), pp. 686–707.

[44] A. Maheshwari, N. G. Paterakis, M. Santarelli, and M. Gibescu. "Optimizing the operation of energy storage using a non-linear lithium-ion battery degradation model". In: *Applied Energy* 261 (2020), p. 114360.

[45] M. Raissi, P. Perdikaris, and G. E. Karniadakis. "Physics-informed neural networks: A deep learning framework for solving forward and inverse problems involving nonlinear partial differential equations". In: *Journal of Computational physics* 378 (2019), pp. 686–707.

[46] Z. Jiang, X. Wang, H. Li, T. Hong, F. You, J. Drgoňa, D. Vrabie, and B. Dong. "Physics-informed machine learning for building performance simulation-A review of a nascent field". In: *Advances in Applied Energy* (2025), p. 100223.

[47] M. Raissi, P. Perdikaris, and G. E. Karniadakis. "Physics informed deep learning (part i): Data-driven solutions of nonlinear partial differential equations". In: *arXiv preprint arXiv:1711.10561* (2017).

[48] F. Wang, Z. Zhai, Z. Zhao, Y. Di, and X. Chen. "Physics-informed neural network for lithium-ion battery degradation stable modeling and prognosis". In: *Nature Communications* 15.1 (2024), p. 4332.

[49] M. Aykol, C. B. Gopal, A. Anapolsky, P. K. Herring, B. van Vlijmen, M. D. Berliner, M. Z. Bazant, R. D. Braatz, W. C. Chueh, and B. D. Storey. "Perspective—combining physics and

machine learning to predict battery lifetime". In: *Journal of The Electrochemical Society* 168.3 (2021), p. 030525.

[50] R. G. Nascimento, M. Corbetta, C. S. Kulkarni, and F. A. Viana. "Hybrid physics-informed neural networks for lithium-ion battery modeling and prognosis". In: *Journal of Power Sources* 513 (2021), p. 230526.

[51] G. Sun, Y. Liu, and X. Liu. "A method for estimating lithium-ion battery state of health based on physics-informed machine learning". In: *Journal of Power Sources* 627 (2025), p. 235767.

[52] S. Wang, R. Zhou, Y. Ren, H. Liu, Y. Lin, and C. Lian. "A generalizable physics-informed neural network for lithium-ion battery SOH estimation utilizing partial charging segments". In: *Journal of Energy Chemistry* (2025).

[53] E. Hu, H. H. Choo, W. Zhang, A. Sumboja, I. T. Anggraningrum, A. Z. Syahrial, Q. Zhu, J. Xu, X. J. Loh, H. Pan, et al. "Integrating Machine Learning and Characterization in Battery Research: Toward Cognitive Digital Twins with Physics and Knowledge". In: *Advanced Functional Materials* 35.25 (2025), p. 2422601.

[54] A. Fuller, Z. Fan, C. Day, and C. Barlow. "Digital twin: Enabling technologies, challenges and open research". In: *IEEE access* 8 (2020), pp. 108952–108971.

[55] A. Barré, B. Deguilhem, S. Grolleau, M. Gérard, F. Suard, and D. Riu. "A review on lithium-ion battery ageing mechanisms and estimations for automotive applications". In: *Journal of Power Sources* 241 (2013), pp. 680–689.

[56] J. M. Reniers, G. Mulder, and D. A. Howey. "Review and performance comparison of mechanical-chemical degradation models for lithium-ion batteries". In: *Journal of The Electrochemical Society* 166.14 (2019), A3189–A3200.

[57] J. Cao, D. Harrold, Z. Fan, T. Morstyn, D. Healey, and K. Li. "Deep reinforcement learning-based energy storage arbitrage with accurate lithium-ion battery degradation model". In: *IEEE Transactions on Smart Grid* 11.5 (2020), pp. 4513–4521.

[58] S. Park, A. Pozzi, M. Whitmeyer, H. Perez, A. Kandel, G. Kim, Y. Choi, W. T. Joe, D. M. Raimondo, and S. Moura. "A deep reinforcement learning framework for fast charging of Li-ion batteries". In: *IEEE Transactions on Transportation Electrification* 8.2 (2022), pp. 2770–2784.

[59] M. Dubarry and D. Beck. "Big data training data for artificial intelligence-based Li-ion diagnosis and prognosis". In: *Journal of Power Sources* 479 (2020), p. 228806.

[60] S. M. Rezvanizaniani, Z. Liu, Y. Chen, and J. Lee. "Review and recent advances in battery health monitoring and prognostics technologies for electric vehicle (EV) safety and mobility". In: *Journal of power sources* 256 (2014), pp. 110–124.

[61] W. Hua, B. Stephen, and D. C. Wallom. "Digital twin based reinforcement learning for extracting network structures and load patterns in planning and operation of distribution systems". In: *Applied Energy* 342 (2023), p. 121128.

[62] R. Subramanya, S. A. Sierla, and V. Vyatkin. "Exploiting battery storages with reinforcement learning: a review for energy professionals". In: *IEEE Access* 10 (2022), pp. 54484–54506.

[63] Z. Jiang, X. Wang, and B. Dong. "Physics-informed modularized neural network for advanced building control by deep reinforcement learning". In: *Advances in Applied Energy* (2025), p. 100237.

[64] H. Hoshino and Y. Nakahira. "Physics-informed RL for maximal safety probability estimation". In: *2024 American Control Conference (ACC)*. IEEE. 2024, pp. 3576–3583.

[65] T. Zhu, H. Wang, Z. Cao, J. Xi, and Y. Wen. "Towards Intelligent Battery Management via A Five-Tier Digital Twin Framework". In: *arXiv preprint arXiv:2509.02366* (2025).